AMERICAN SOCIETY FOR MICROBIOLOGY | Journal of Virology®

VIRUS-CELL INTERACTIONS

Pseudorabies Virus US3-Induced Tunneling Nanotubes Contain Stabilized Microtubules, Interact with Neighboring Cells via Cadherins, and Allow Intercellular Molecular Communication

Robert J. J. Jansens,[a] Wim Van den Broeck,[b] Steffi De Pelsmaeker,[a] Jochen A. S. Lamote,[a] Cliff Van Waesberghe,[a] Liesbeth Couck,[b] Herman W. Favoreel[a]

Department of Virology, Parasitology and Immunology[a] and Department of Morphology,[b] Faculty of Veterinary Medicine, Ghent University, Belgium

ABSTRACT Tunneling nanotubes (TNTs) are long bridge-like structures that connect eukaryotic cells and mediate intercellular communication. We found earlier that the conserved alphaherpesvirus US3 protein kinase induces long cell projections that contact distant cells and promote intercellular virus spread. In this report, we show that the US3-induced cell projections constitute TNTs. In addition, we report that US3-induced TNTs mediate intercellular transport of information (e.g., green fluorescent protein [GFP]) in the absence of other viral proteins. US3-induced TNTs are remarkably stable compared to most TNTs described in the literature. In line with this, US3-induced TNTs were found to contain stabilized (acetylated and detyrosinated) microtubules. Transmission electron microscopy showed that virus particles are individually transported in membrane-bound vesicles in US3-induced TNTs and are released along the TNT and at the contact area between a TNT and the adjacent cell. Contact between US3-induced TNTs and acceptor cells is very stable, which correlated with a marked enrichment in adherens junction components beta-catenin and E-cadherin at the contact area. These data provide new structural insights into US3-induced TNTs and how they may contribute to intercellular communication and alphaherpesvirus spread.

IMPORTANCE Tunneling nanotubes (TNT) represent an important and yet still poorly understood mode of long-distance intercellular communication. We and others reported earlier that the conserved alphaherpesvirus US3 protein kinase induces long cellular protrusions in infected and transfected cells. Here, we show that US3-induced cell projections constitute TNTs, based on structural properties and transport of biomolecules. In addition, we report on different particular characteristics of US3-induced TNTs that help to explain their remarkable stability compared to physiological TNTs. In addition, transmission electron microscopy assays indicate that, in infected cells, virions travel in the US3-induced TNTs in membranous transport vesicles and leave the TNT via exocytosis. These data generate new fundamental insights into the biology of (US3-induced) TNTs and into how they may contribute to intercellular virus spread and communication.

KEYWORDS pseudorabies virus, PRV, herpes, US3, tunneling nanotubes, TNT, cadherins, microtubules, pseudorabies

Received 3 May 2017 **Accepted** 16 July 2017

Accepted manuscript posted online 26 July 2017

Citation Jansens RJJ, Van den Broeck W, De Pelsmaeker S, Lamote JAS, Van Waesberghe C, Couck L, Favoreel HW. 2017. Pseudorabies virus US3-induced tunneling nanotubes contain stabilized microtubules, interact with neighboring cells via cadherins, and allow intercellular molecular communication. J Virol 91:e00749-17. https://doi.org/10.1128/JVI.00749-17.

Editor Richard M. Longnecker, Northwestern University

Address correspondence to Herman W. Favoreel, herman.favoreel@ugent.be.

In 2004, the term tunneling nanotubes (TNTs) was coined to describe actin-containing membranous conduits that connected neighboring cells in PC12 cell cultures (1). In PC12 cells, TNTs were shown to transfer membrane-linked proteins and vesicles. Soon

afterward, it was discovered that these structures represent a new and widespread communication system in eukaryotic cells that contributes to immunological processes (2), development of multicellular organisms (3), and tissue regeneration (4). It became clear that TNTs are able to mediate the transport of a large variety of cargo, including proteins (5), organelles (6), and signals that lead to depolarization of membrane potential (7).

Not surprisingly, TNTs were found to be important in several diseases. For example, TNTs were shown to mediate transport of misfolded proteins, which may contribute to the development of Alzheimer's disease, Huntington's disease, and transmissible spongiform encephalopathies (8–10). They have also been shown to connect breast cancer cells, allowing the transport of P-glycoprotein, a membrane protein that mediates multidrug resistance (11). Certain viruses have been reported to use TNTs to spread more efficiently between cells. Retroviruses, including HIV, are able to use existing TNTs between T cells to spread from infected to uninfected T cells (12). In macrophages, HIV is able to trigger the formation of TNTs via its Nef protein (13). More recently, members of the *Paramyxoviridae*, *Orthomyxoviridae*, and *Arteriviridae* were shown to use TNTs for intercellular spread (14–16). Infection with these viruses also increases the number of TNT-connected cells, although the responsible viral factors have not yet been identified. Furthermore, several members of the *Alphavirus* genus of the *Togaviridae* are able to induce the formation of TNTs in several cell types. This induction of TNTs is dependent on both the E2 envelope glycoprotein and the Cp capsid protein, but the cellular pathways through which they act are still unknown (17).

We and others have reported that pseudorabies virus (PRV) and other (alpha)herpesviruses induce the formation of long actin- and microtubule-containing cell projections that make contact with distant cells and that these structures are associated with enhanced intercellular virus spread (18–22). For PRV and other alphaherpesviruses, cell projection formation depends on the conserved viral US3 serine/threonine protein kinase. To trigger cell projection formation, US3 modulates cytoskeleton-controlling cellular Rho-GTPase signaling pathways, particularly through activation of group I p21-activated kinases (PAK) and suppression of RhoA signaling (23, 24).

Our earlier reports indicated that US3-induced cell projections are remarkably stable for up to several days and that they are very tightly and stably associated with connected neighboring cells, despite migration of both the US3-expressing and contacted cells (23, 24). From the current study, we report that US3-induced cell projections constitute TNTs. In addition, we show that microtubules inside the US3-induced TNTs display stabilizing posttranslational modifications (PTMs), that cadherin adhesion molecules are present in the contact area between a cell projection and the neighboring cell, and that US3-induced TNTs allow intercellular passage of biomolecules, even in the absence of other viral proteins. Also, we show that in infected cells, US3-induced TNTs contain virions that are individually packaged in transport vesicles.

RESULTS

US3-induced projections are tunneling nanotubes and allow intercellular spread of biomolecules in the absence of other viral proteins. Cell projections are classified as tunneling nanotubes (TNTs) based on a number of criteria (25, 26): TNTs are intercellular structures that (i) form a straight connection between cells by a membranous conduit, (ii) contain actin filaments and in some cases also microtubules, (iii) lack contact with the underlying substrate on which the cells are grown (thus forming a bridge between cells), and (iv) allow direct intercellular communication via transport of molecules or organelles. To assess whether US3-induced cell projections fulfill the first three of these criteria, swine testicle (ST) cells were transfected with a plasmid encoding US3 of PRV, stained using phalloidin-Texas Red (TR) to visualize the actin cytoskeleton, and analyzed by confocal microscopy. Figure 1A to C and Movie S1 in the supplemental material show that US3-induced cell projections indeed generate straight and actin-containing cellular connections between cells that lack contact with the underlying

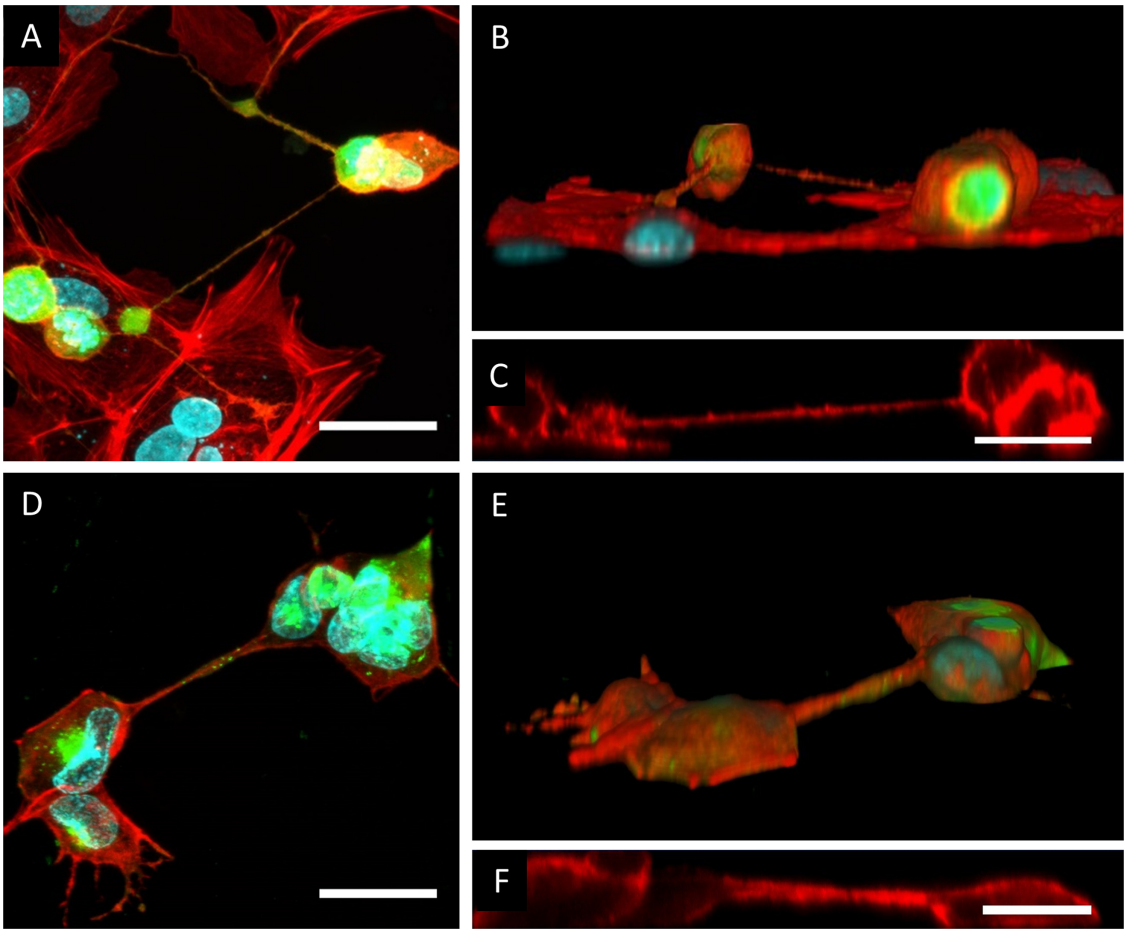

FIG 1 US3-induced cell projections are tunneling nanotubes (TNTs). (A to C) Confocal image of cell projections in US3-transfected ST cells showing GFP cotransfected with US3 (green), filamentous F-actin (red), and nuclei (cyan). (A) Maximum projection image of different *xy* optical sections through the sample, showing the presence of F-actin in US3-induced cell projections. Bar, 30 μm. (B and C) Three-dimensional (3D) reconstruction (B) and *xy* section (C) of the same confocal image, showing that the US3-induced cell projections do not make contact with the underlying substrate. Bar, 20 μm. (D to F) Confocal image of cell projections in PRV-infected ST cells showing viral gD protein (green), filamentous F-actin (red), and nuclei (cyan). (D) Maximum projection image of different *xy* optical sections through the sample, showing the presence of F-actin in PRV-induced cell projections. Bar, 30 μm. (E and F) 3D reconstruction (E) and *xz* section (F) of the same confocal image, showing that the PRV-induced cell projections do not make contact with the underlying substrate. Bar, 20 μm.

substrate, confirming the first three criteria associated with TNTs. These observations were also confirmed in PRV-infected cells (Fig. 1D to F).

As a fourth criterion, TNTs allow direct intercellular communication via transport of molecules/organelles. Although earlier research had shown that in PRV-infected cells, US3-induced cell projections promote virus spread, it had not yet been investigated whether US3-induced cell projections allow direct intercellular communication in the absence of other viral proteins. By live-cell imaging of cells cotransfected with US3 and green fluorescent protein (GFP), we found that US3-transfected cells are able to pass on the GFP signal to connected cells (Fig. 2A; see also Movie S2), which was not the case upon cotransfection of GFP with kinase-inactive US3, which is unable to generate cell projections (data not shown). Transport of GFP via US3-induced cell projections was also confirmed using a coculture system. Here, a donor ST cell population was stained with the cytoplasmic tracer CellTrace violet and cotransfected with GFP and active US3 or kinase-inactive US3. The acceptor population was stained with the membrane probe Did. These populations were then cultured together in a 1:1 ratio for 48 h. Using wild-type US3, GFP/Did doubly positive (green and magenta) cells could be observed (Fig. 2B). Using kinase-inactive US3, on the other hand, no GFP/Did doubly positive cells

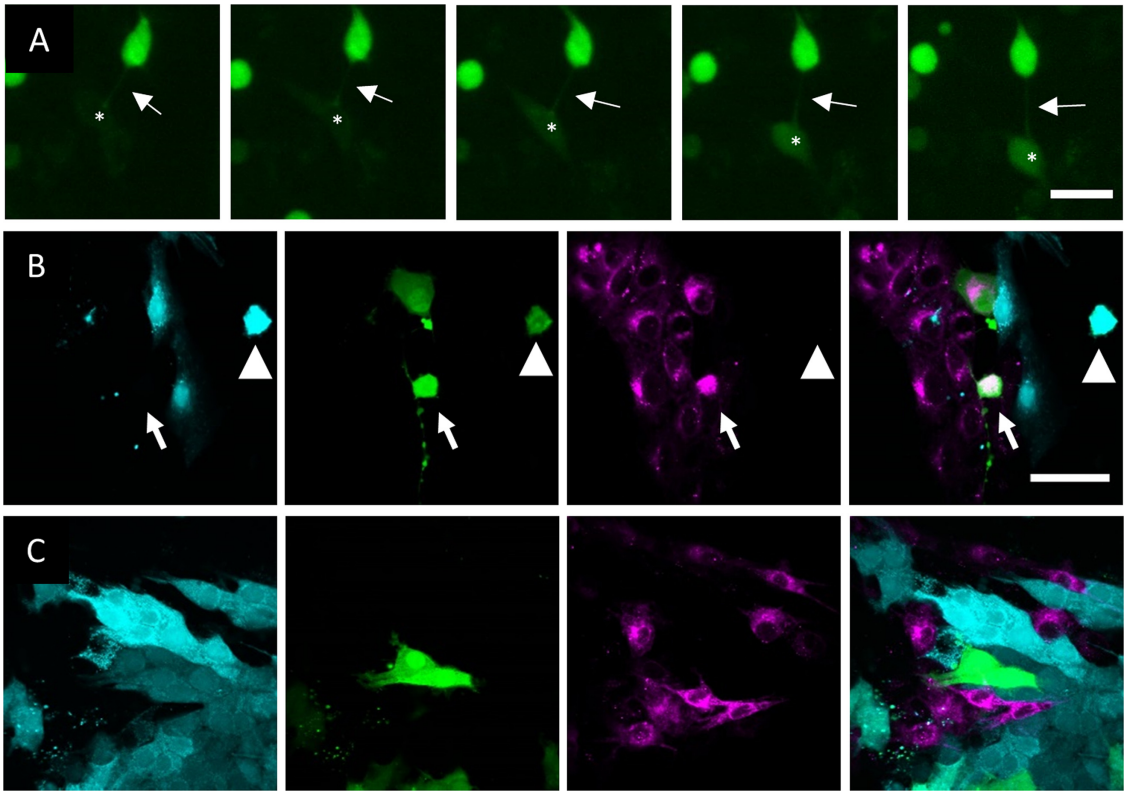

FIG 2 US3-induced cell projections allow transport of GFP signal from transfected to untransfected cells. (A) GFP signal is transferred from US3/GFP-cotransfected ST cells to nontransfected ST cells. Arrows show a TNT connecting a US3/GFP-transfected cell to a nontransfected cell. Asterisks show the location of an acceptor cell that becomes GFP positive over time. The interval between each frame and the next is 30 min. Bar, 30 μm. Images represent stills from a time lapse video (Movie S2). (B) Coculture experiment results showing transfer of GFP (green) from a wild-type US3/GFP-transfected CellTrace violet-stained (cyan) donor population (arrowhead) to a nontransfected Did-stained (magenta) accepter population (arrow). (C) Use of the same experimental setup as that described for panel B but using kinase-inactive US3 instead of wild-type US3 did not lead to GFP transfer to nontransfected cells. Bar (for panels B and C), 50 μm.

could be found (Fig. 2C). To analyze whether extracellular transport, e.g., via exosomes, possibly contributed to GFP spread from the US3-expressing donor cells to the Did-positive acceptor cell population, a control experiment was performed in which the supernatant of cells cotransfected with US3 and GFP was transferred to untransfected cells. This did not lead to transfer of GFP to the acceptor cells (data not shown). In conclusion, US3-induced cell projections can be classified as TNTs and allow intercellular passage of biomolecules.

US3-induced tunneling nanotubes contain stabilized microtubules. Most tunneling nanotubes described in the literature are highly fragile and have an average life span of a few minutes to a few hours (1, 4, 26). However, live-cell imaging experiments showed that US3-induced tunneling nanotubes are remarkably stable, often remaining intact for the entire duration of the experiment, i.e., 24 h. This observation led us to investigate the presence of posttranslational modifications (PTMs) of tubulin that have a stabilizing effect on microtubules. We investigated the presence of two reversible PTMs: acetylated tubulin, a PTM commonly associated with stable microtubules and increased transport along microtubules (27), and detyrosinated tubulin, another PTM that is highly associated with stable microtubules and that has been shown to increase the affinity of the motor protein kinesin for microtubules (27). We also investigated the presence of Δ2 tubulin, a nonreversible PTM that is mainly found in terminally differentiated axons (28). Immunostaining of US3-transfected cells showed that 52% ± 6% of US3-induced TNTs contained acetylated tubulin (Fig. 3A) and that 91% ± 2% contained detyrosinated tubulin (Fig. 3B). In contrast, Δ2 tubulin could not be detected

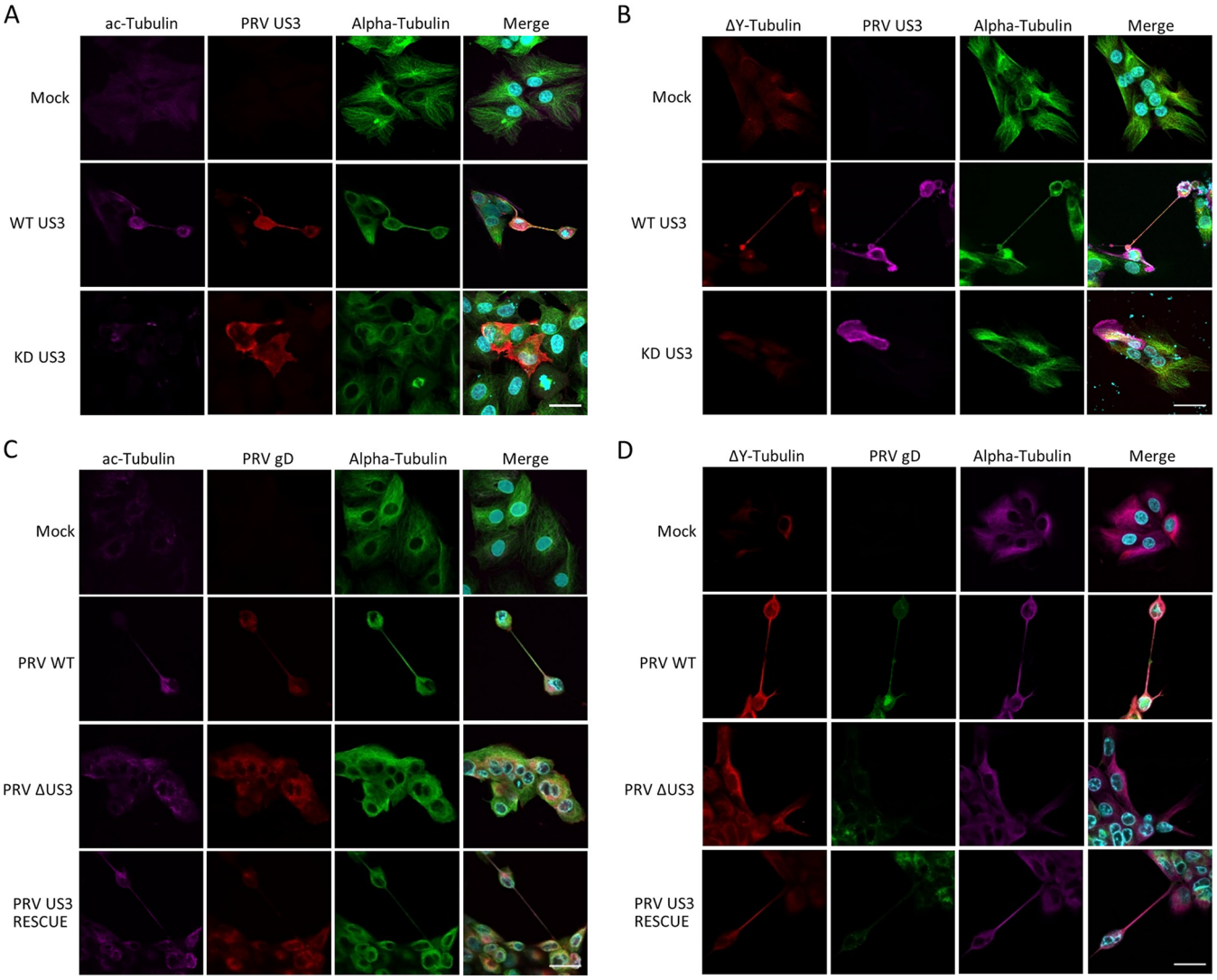

FIG 3 US3-induced TNTs contain stabilized microtubules. TNTs induced in US3-transfected ST cells (A and B) or PRV-infected ST cells (C and D) contain acetylated (A and C) and detyrosinated (B and D) tubulin. (A) Magenta, acetylated tubulin; red, PRV US3; green, tubulin; cyan, nuclei. (B) Red, detyrosinated tubulin; magenta, US3; green, tubulin; cyan, nuclei. (C) Magenta, acetylated tubulin; red, PRV gD; green, tubulin; cyan, nuclei. (D) Red, detyrosinated tubulin; green, PRV gD; magenta, tubulin; cyan, nuclei. Bars, 30 μm. KD, kinase dead; WT, wild type; PRV, pseudorabies virus; ΔUS3, US3null mutant.

(data not shown). To determine whether these observations also hold true in virus-infected cells, cells were either subjected to mock infection or infected with wild-type PRV, an isogenic US3null mutant, or a US3 rescue virus. Immunostaining again showed the presence of both acetylated tubulin (Fig. 3C) and detyrosinated tubulin (Fig. 3D) in the US3-induced TNTs. In conclusion, we showed that microtubules in US3-induced TNTs are actively stabilized and contain PTMs, which have been reported to promote microtubule motor-based transport.

The contact area between US3-induced tunneling nanotubes and contacted neighboring cells is enriched in components of adherens junctions. Live-cell imaging experiments (see, e.g., Movie S2) showed that the interaction between US3-induced TNTs and the contacted neighboring cells is very stable. Indeed, intercellular contacts often remain intact despite substantial migration and movement of both the donor cell and the acceptor cell. This suggests that adhesion molecules may be present and enriched at the contact area between the TNT and the acceptor cell. Therefore, we investigated the presence of adherens junction components E-cadherin and beta-catenin in the contact area (29). Because of a lack of antibodies that cross-react with

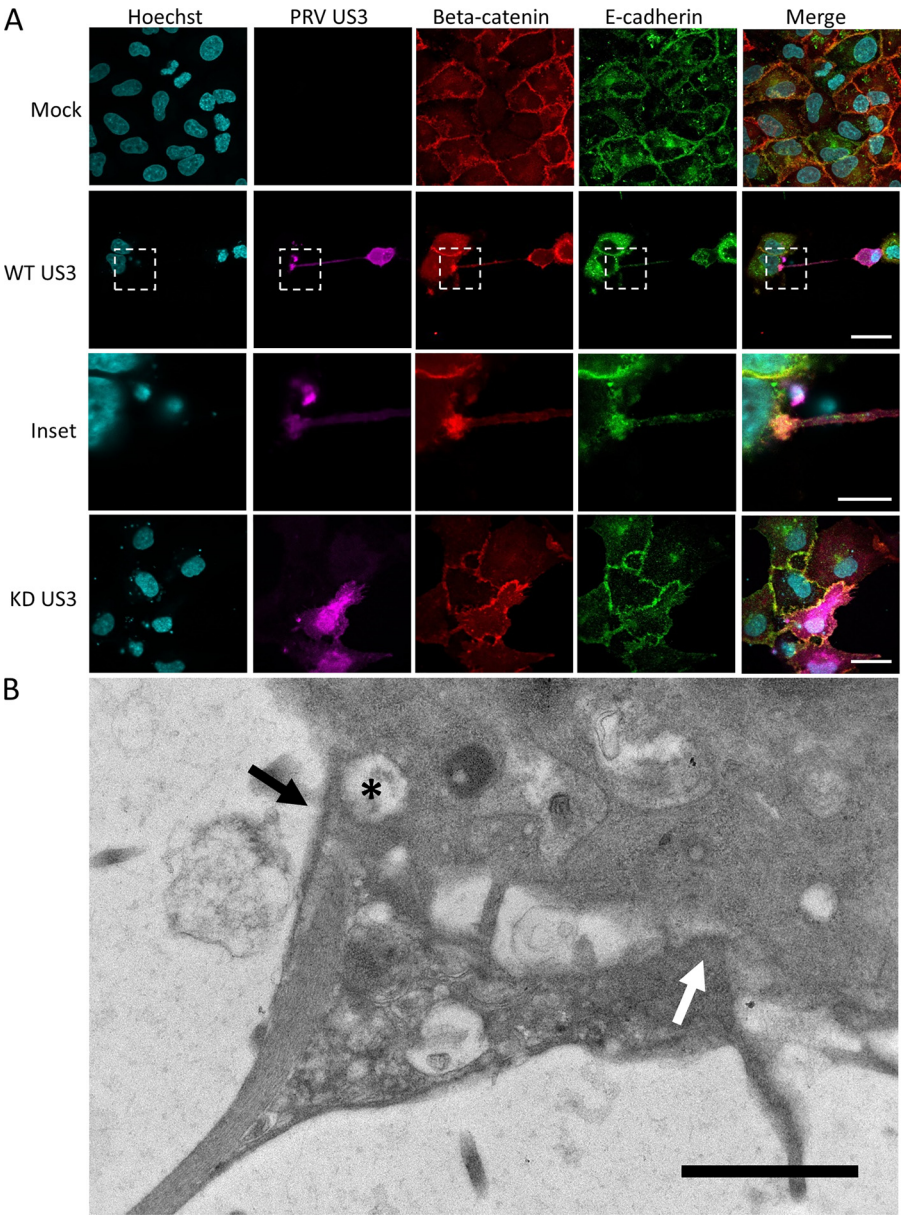

FIG 4 The contact area between US3-induced TNTs and acceptor cells is enriched in E-cadherin and beta-catenin in transfected cells and has a heterogeneous structure. (A) E-cadherin (green) and beta-catenin (red) staining in US3-transfected (magenta) RK13 cells. Bars, 30 μm; inset bar, 10 μm. (B) Transmission electron microscopy (TEM) image of an area of contact between a TNT and acceptor cell in US3-transfected ST cells. An area with loose contact is indicated with a white arrow, while an area with apparent cytoplasmic connectivity between the two cells is indicated with a black arrow. A vesicle appears to be transported through this region with cytoplasmic connectivity (black asterisk). Bar, 1 μm. KD, kinase dead; WT, wild type.

porcine E-cadherin, rabbit RK13 cells were used to investigate whether beta-catenin and E-cadherin were enriched in the contact area of US3-induced TNTs. Earlier studies had already showed that US3 also induces cell projections in RK13 cells (18). Immunostaining of RK13 cells transfected with US3 indeed showed the accumulation of both E-cadherin and beta-catenin at the contact area between the TNT and the acceptor cell (Fig. 4A). The contact area between the US3-induced TNT and the contacted cells was further resolved by transmission electron microscopy (TEM). TEM analysis of US3-transfected ST cells indicated heterogeneity in the contact area between US3-induced TNTs and acceptor cells, including regions of relatively loose contact and regions that showed cytoplasmic connectivity between the two cells (Fig. 4B). Interestingly, regions

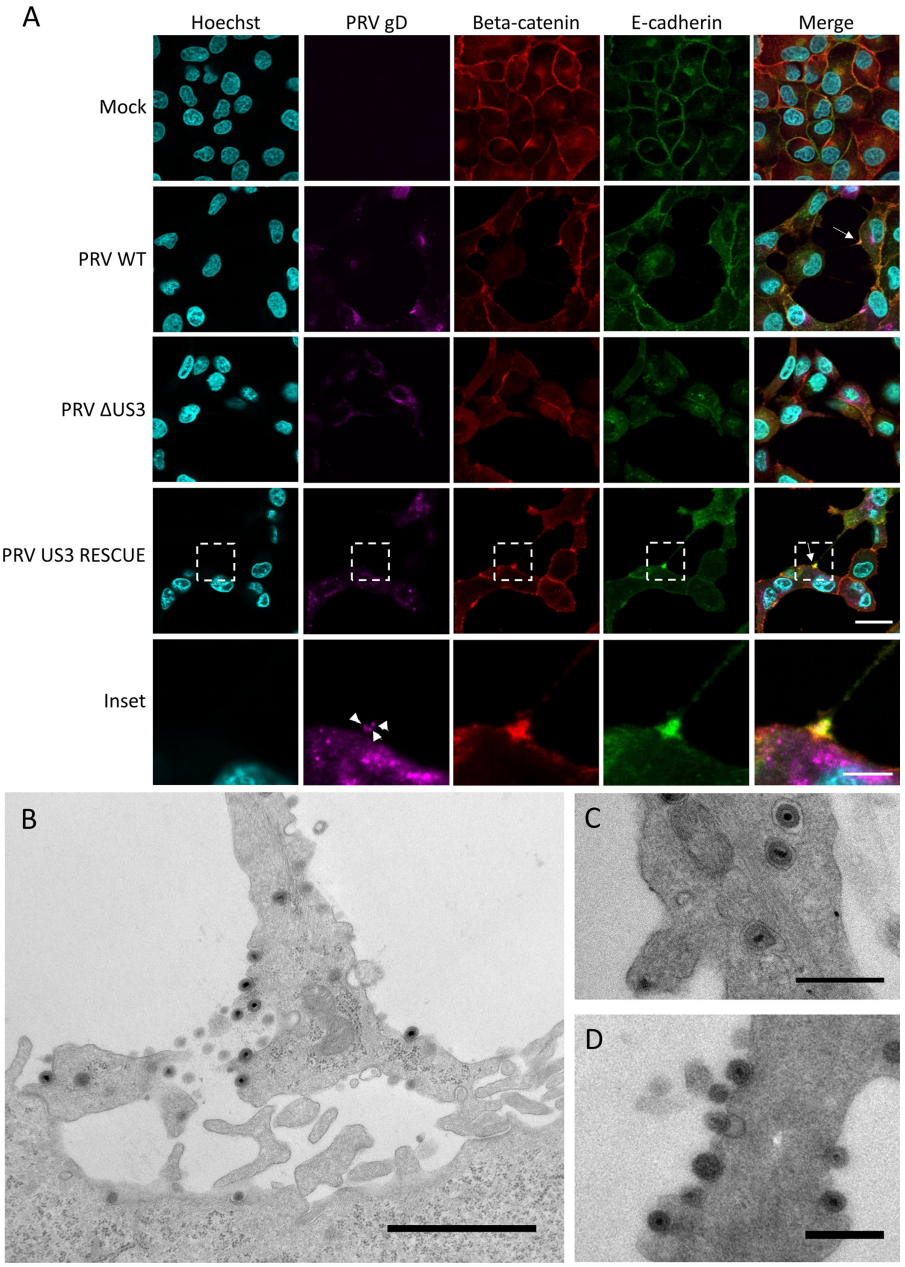

FIG 5 The contact area between US3-induced TNTs and acceptor cells in PRV-infected samples is enriched in E-cadherin and beta-catenin, and enveloped virus is present in vesicles in the TNTs and is released along the length of the TNT and at the contact zone. (A) E-cadherin (green) and beta-catenin (red) staining in PRV-infected (magenta) RK13 cells. White arrows show areas enriched in beta-catenin and E-cadherin. Arrowheads indicate punctate gD signal in the contact zone, indicating the presence of virus particles. Bars, 30 μm; inset bar, 10 μm. (B to D) Transmission electron microscopy (TEM) images of ST cells infected with wild-type PRV. (B) Contact area of a US3-induced TNT with a nearby cell in ST cells infected with PRV. Bar, 1,500 nm. (C to D) Virus particles are transported through TNTs as individually membrane-wrapped enveloped virions and are released over the entire length of the conduit. Bars, 500 nm. WT, wild type; PRV, pseudorabies virus; ΔUS3, US3null mutant.

with apparent cytoplasmic connectivity were sometimes associated with small vesicles that appeared to be transported from one cell to the other (asterisks in Fig. 4B).

These immunofluorescence and TEM findings were confirmed in virus-infected cells. Immunofluorescence assays again indicated an obvious enrichment of both beta-catenin and E-cadherin in the contact area between TNTs and acceptor cells (Fig. 5A). Costaining of the viral gD envelope protein showed discrete punctae that likely

represent PRV virions moving through the TNTs. An earlier report already showed movement of PRV particles in US3-induced cell projections, using a PRV strain in which the VP26 capsid protein was fused to GFP, which does not allow discrimination between enveloped particles and naked capsids (18). The gD staining data suggest that virions are transported in TNTs as enveloped virus particles.

TEM imaging of PRV-infected cells showed that the structure of the contact area was similar to that observed in US3-transfected cells (Fig. 5B). TEM analysis further confirmed that the virions that were transported in the TNTs were enveloped and not naked capsids. Interestingly, enveloped virions in the TNTs could be observed in close proximity to filamentous structures, likely representing microtubules (Fig. 5C). Virions were almost invariably individually packaged in transport vesicles. Exocytosis of virions was observed over the entire length of the TNT, including at the contact area (Fig. 5D). This indicates that virions likely do not transfer directly from the TNT to the acceptor cell but undergo the process of exocytosis followed by fusion with the plasma membrane of the contacted cell. This is in line with the general observation that alphaherpesviruses that lack the gB fusion envelope protein are unable to spread between cells (30), even though cells infected with gBnull PRV still form US3-induced TNTs that contain enveloped virions (data not shown).

In conclusion, components of adherens junctions are enriched in the contact area of US3-induced TNTs and connected cells in both US3-transfected cells and PRV-infected cells. TEM analysis showed that the contact area has a heterogeneous structure with zones of apparently relatively loose contact, zones with intense contact, and zones where (perhaps transient) fusion allows transport of cargo. PRV is transported through the TNTs as enveloped virions that are individually wrapped in transport vesicles and are released over the entire length of the TNT and at the contact area.

Mitochondria are transported in US3-induced tunneling nanotubes. Organelle transport, particularly mitochondrion transport, has been described in several TNTs (6, 31). We investigated whether this is also the case in US3-induced TNTs. MitoTracker Red CMXRos staining showed that mitochondria are present in about half of the TNTs in US3-transfected cells (Fig. 6A and E). On average, 1.3 $\pm$ 0.1 mitochondria were observed in TNTs of US3-transfected cells. To investigate whether mitochondria undergo active transport in TNTs, live-cell imaging experiments were performed. Mitochondria could be seen moving, typically from the connected cell toward the transfected cell (Fig. 6B; see also Movie S3), which is in line with other reports on mitochondrion transport in TNTs (32). Net transport of mitochondria in TNTs of transfected cells occurred at an average speed of 6.7 $\pm$ 7.5 nm s^{-1}, which is similar to the speed of mitochondrion transport previously described in TNTs in PC12 cells (32).

Analogous experiments were performed in virus-infected cells. Confocal microscopy and TEM confirmed the presence of mitochondria in virus-induced TNTs (Fig. 6C and data not shown). TNTs formed by PRV-infected cells contained on average 4.7 $\pm$ 0.4 mitochondria per TNT, which is considerably more than in transfected cells (Fig. 6C and E). Mitochondrial transport was also observed by live-cell imaging at a significantly higher speed ($P < 0.05$) than in transfected cells: 10.1 $\pm$ 1.1 nm s^{-1} (Fig. 6D). These observations show that US3-induced TNTs contain dynamic mitochondria, particularly in virus-infected cells.

DISCUSSION

In this study, we showed that cell projections induced by the US3 protein kinase of PRV constitute TNTs. Without the need for expression of other viral proteins, US3-induced TNTs allow intercellular spread of GFP. US3-induced TNTs contain dynamic mitochondria and microtubules that are posttranslationally modified by acetylation and detyrosination. The contact area between the TNTs and connected cells is enriched in adherens junction molecules beta-catenin and E-cadherin.

US3-induced TNTs are remarkably long-living, compared to most TNTs described in the literature (26, 33). In this paper, we describe a possible characteristic of US3-induced TNTs that may help to explain this. We showed that US3-induced TNTs contain

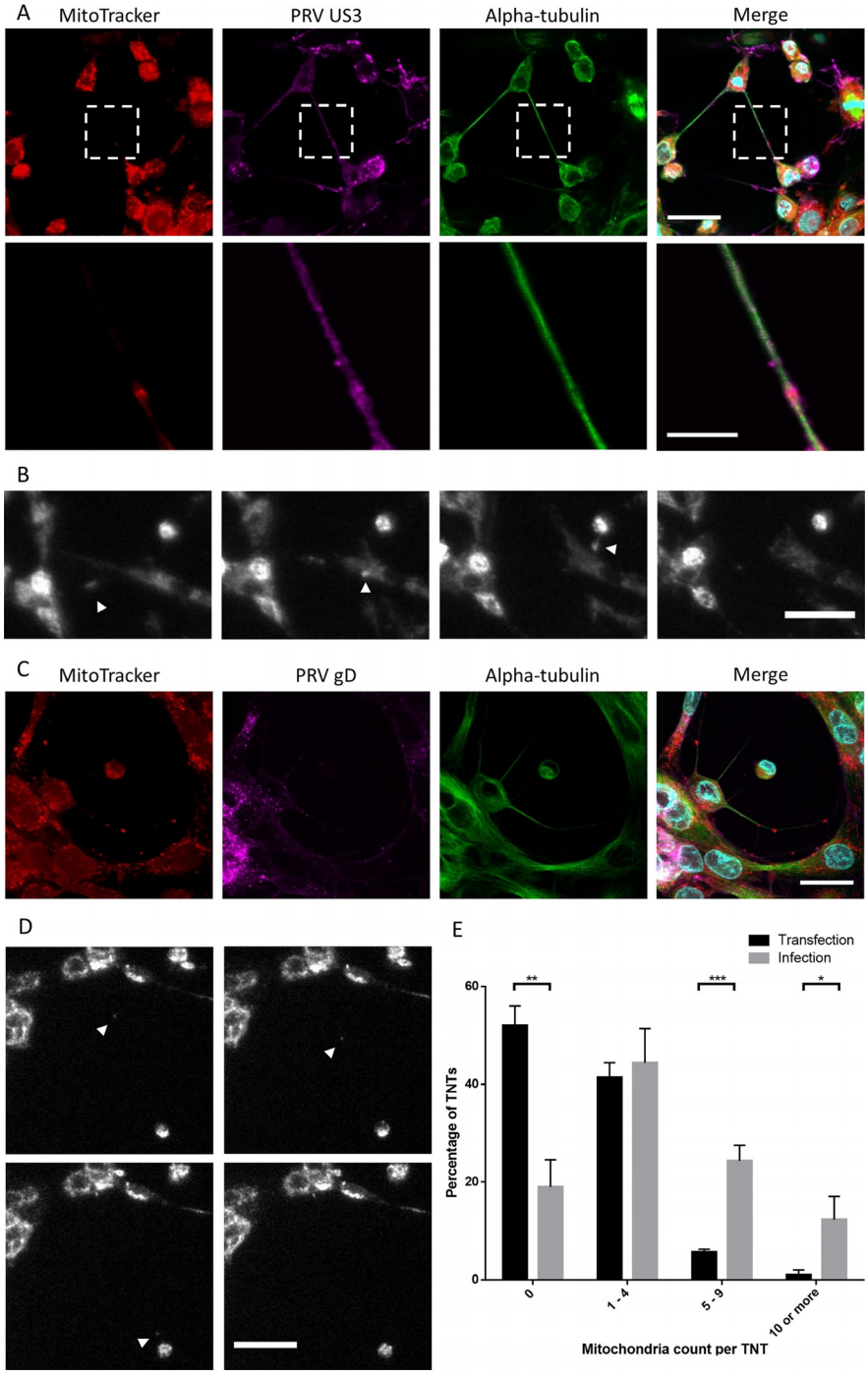

FIG 6 Dynamic mitochondria are present in US3-induced TNTs in both US3-transfected cells and PRV-infected cells. (A) Mitochondrion (red) staining in US3-transfected (magenta) ST cells shows the presence of mitochondria in US3-induced TNTs. (B) Mitochondria are transported in TNTs in US3-transfected cells. White arrowheads show mitochondria transported in a TNT in the direction from a connected cell to a transfected cell. The interval between each frame and the next is 20 min. Bar, 30 μm. Images represent stills from a time lapse video (Movie S3). (C) Mitochondrion (red) staining in PRV-infected (magenta) ST cells shows the presence of mitochondria in TNTs. (D) Mitochondria are transported in TNTs in PRV-infected cells. White arrowheads show mitochondria transported in a TNT. The sequence is from upper left to bottom right. The interval between each frame and the next is 20 min. Bar, 30 μm. Images represent stills from a time lapse video (Movie S4). (E) Quantification of mitochondria present in US3-induced TNTs in transfected cells versus infected cells. Black bars show the number of mitochondria per TNT in US3-transfected cells. Gray bars show the number of mitochondria per TNT in PRV-infected cells. Error bars show standard deviations, with a single asterisk (*) indicating *P* values of <0.05, double asterisks (**) indicating *P* values of <0.01, and triple asterisks (***) indicating *P* values of <0.001.

microtubules that are posttranslationally modified by acetylation and detyrosination. Acetylated tubulin is a hallmark of microtubule stabilization and is associated with an increased level of microtubule-mediated transport (34). Detyrosinated tubulin is also enriched in stable microtubules, and it has been shown that kinesin-1 preferentially binds detyrosinated tubulin over tyrosinated tubulin (34, 35). A US3-dependent stabilization of microtubules has previously been shown for herpes simplex virus 1 (36), which is in line with our current observations. Detyrosinated tubulin can be further modified into the irreversible modification Δ2-tubulin. Interestingly, no Δ2-tubulin was detected in cells expressing PRV US3. This shows that tubulin modified in response to US3 expression remains part of the reversible detyrosination/retyrosination cycle, in contrast to microtubules in axons, which are irreversibly modified (28).

Another characteristic of US3-induced TNTs that may help to explain their stability is the enrichment of beta-catenin and E-cadherin in the area of contact of US3-induced TNTs with acceptor cells. Both of these proteins are components of adherens junctions and mediate firm cell-cell contact in a calcium-dependent way. The presence of components of adherence junctions in the contact area of endogenous TNTs in different cell types was shown previously (37, 38). Nevertheless, US3-induced TNTs and their contact with acceptor cells were resistant to EDTA/trypsin treatment (data not shown). A similar observation was made for TNTs connecting PC12 cells (1). The presence of beta-catenin and E-cadherin is likely important to stabilize the (initial) contact between a TNT and a connected cell, whereas other elements, e.g., (micro)fusion events, may subsequently lead to calcium-independent contact between the TNT and the acceptor cell.

The structure of the area of contact of TNTs with acceptor cells has long been a topic of discussion within the field (7, 39). Although the idea is speculative at this stage, our observations may be in line with a model in which (transient) microfusions between donor and acceptor cell membranes at the contact area allow intercellular transport of biomolecules. This hypothesis is supported by the observation of vesicles apparently transporting through the contact area observed by electron microscopy. However, the inherently static nature of electron microscopy makes it impossible to draw firm conclusions about apparent dynamic processes. In any case, we found that US3-induced TNTs allow transport of GFP signal from donor to acceptor cells without the need for expression of other viral proteins. Interestingly, in a coculture system, transfer of the GFP signal was not associated with transfer of the cytoplasmic marker dye CellTrace violet (Fig. 2B). This could be an indication that GFP is not transported in the form of protein but as DNA or mRNA. In future experiments, it will be interesting to assess exactly which types of biomolecules can be transferred between cells via US3-induced TNTs.

Mitochondria were found to be present and to migrate in TNTs both in infected cells and in transfected cells. The number of mitochondria was higher in TNTs in PRV-infected cells than in TNTs in US3-transfected cells, and the speed of mitochondrion movement was also significantly higher in TNTs in infected cells versus transfected cells and was in the range of the speed of mitochondrion movement observed in other TNTs (32). Although it is currently unclear if dynamic mitochondria are involved in growth of US3-induced TNTs and/or virus spread along these structures, it is interesting that PRV has been reported before to alter mitochondrial dynamics in neuronal axons and that this is important for virus spread in axons (40). In axons, the effect of PRV on the mitochondrial dynamics was mediated through the Miro GTPase. It was also shown that expression of a Miro mutant that is unable to disrupt mitochondrial dynamics results in smaller PRV plaques in nonneuronal cells, indicating that disruption of mitochondrial dynamics is also important for PRV infection in nonneuronal cells. Miro1 has been shown to regulate the transport of mitochondria between nonneuronal cells through TNTs (31). It would therefore be interesting to investigate whether and how PRV interacts with this GTPase and how this affects the formation of and transport through US3-induced TNTs.

Our data indicate that direct intercellular transport of virus particles from donor to

acceptor cells is unlikely. Indeed, our TEM analyses showed that virions in TNTs invariably were carried in membrane-bound vesicles, often packaged as individual virus particles. In order to initiate infection in the acceptor cell, these packaged virions need to lose the vesicle membrane and the viral envelope. This suggests that the virions need to leave the donor cell via exocytosis, losing the vesicle membrane, and subsequently need to infect the acceptor cell by fusing the viral envelope with the acceptor cell membrane. In line with this, our TEM assays showed virion exocytosis along the TNTs, including at the narrow contact area between a donor cell and an acceptor cell. These results are also in line with the fact that viral spread, including that occurring via US3-induced TNTs, does not occur in the absence of the viral envelope proteins that are essential for fusion of the envelope with the host cell membrane (41) (data not shown).

In conclusion, the current report shows that the cell projections induced by the PRV US3 protein kinase constitute TNTs that allow intercellular transport of molecular information, e.g., GFP, without the need for expression of other viral proteins. US3-induced TNTs contain microtubules with stabilizing posttranslation modifications and dynamic mitochondria. E-cadherin and beta-catenin are enriched at the contact area between the TNTs and surrounding cells. Virions are transported via the TNTs as individually membrane-wrapped enveloped virions and are released from the TNT via exocytosis. Our findings help to explain the remarkable longevity of US3-induced TNTs, which renders them a unique model to study TNT biology. In addition, the finding that US3-induced TNTs allow intercellular transport of biological information (e.g., GFP) in the absence of other viral proteins indicates that these structures may serve functions that stretch beyond direct intercellular virus spread and may open avenues toward manipulation of this system to create tools that promote intercellular communication.

MATERIALS AND METHODS

Cells and viruses. Swine testicle (ST) cells were cultured in minimal essential medium (MEM; Gibco) supplemented with 10% fetal calf serum (FCS), 1 mM sodium pyruvate, 10^5 U/liter penicillin, 100 mg/liter streptomycin, and 50 mg/liter gentamicin. Rabbit kidney cells (RK13) were cultured in MEM supplemented with 10% FCS, 10^5 U/liter penicillin, 100 mg/liter streptomycin, and 50 mg/liter gentamicin. Subconfluent cells were infected at a multiplicity of infection (MOI) of 10 and fixed at 7 h postinfection (hpi) as previously described (18). Wild-type NIA3, an isogenic US3null mutant, and the corresponding rescue virus were previously described (42, 43) and were kindly donated by the ID-DLO (The Netherlands).

Transfections and coculture. Cells were transfected with 750 ng of plasmid DNA using JetPrime (Polyplus transfection) according to the manufacturer's instructions. For cotransfections, equal amounts of both plasmids were transfected. Cotransfection of a US3-encoding plasmid and a GFP-encoding plasmid leads to >95% doubly positive cells (44). The plasmid encoding the wild-type NIA3 US3 protein (pKG1) was described previously (45). The plasmid encoding a kinase-inactive US3 protein with a K138Q mutation (pHF61) was described previously (46). The pTrip plasmid encoding enhanced GFP (eGFP) was a kind gift of B. Verhasselt (Ghent University, Ghent, Belgium).

For coculture experiments, cells were first labeled using CellTrace violet or Did, after which they were transfected using JetPrime. At 3 h posttransfection, cells were washed with phosphate-buffered saline (PBS)-EDTA and subjected to trypsinization. Next, they were centrifuged and donor and acceptor population cells were seeded together at a 1:1 ratio in a 24-well plate with insertions coated with type-I collagen (BD Biosciences). The cells were cocultured for 48 h, after which they were fixed and imaged.

Immunofluorescence and dyes. Cells were fixed using 3% paraformaldehyde, after which they were permeabilized using 0.1% Triton X-100. Microtubule stainings were performed as described before (18). Mouse anti-US3 antibody (47) was used at a 1/50 dilution and was a kind gift of Leigh Anne Olsen and Lynn Enquist (Princeton University). Mouse anti-gD antibody was described earlier (48) and was used at a 1/50 dilution. Rabbit anti-detyrosinated tubulin (ab48389), mouse anti-acetylated tubulin (ab24610), and rabbit anti-beta-catenin (ab16051) were purchased from Abcam and were used at dilutions of 1/200, 1/200, and 1/300, respectively. Mouse anti-E-cadherin (CL36) was purchased from BD Biosciences and was used at a 1/100 dilution. Fluorescein isothiocyanate (FITC)-, Texas Red-, or AF647-labeled secondary antibodies were purchased from Thermo Fisher Scientific and were used at 1/200 dilutions.

Mitochondria were stained by incubating cells with 100 nM MitoTracker CMXRos (Thermo Fisher Scientific) in ST culture medium for 30 min. Cells were labeled with CellTrace violet (Thermo Fisher Scientific) according to the manufacturer's instructions. Cells were labeled with Did Vybrant (Thermo Fisher Scientific) according to the manufacturer's instructions.

Stained samples were imaged using a Leica SPE laser scanning confocal microscope (Leica). Live-cell imaging experiments were performed using an Olympus IX81 fluorescence microscope coupled to an Xcellence Pro imaging system (Olympus). Image analysis was performed using FIJI software.

Transmission electron microscopy. Cells were fixed using Karnovski fixative for 1 h at room temperature. Next, the cells were washed four times with a 0.1 M cacodylate buffer, after which a

postfixation step was performed by incubating the cells with a 1% osmium tetroxide solution. The cells were then washed three times with ultrapure water, after which a contrasting step was performed by incubation with 1% uranyl acetate for 1 h. After four washes with ultrapure water were performed, the samples were dehydrated using a series of graded alcohol concentrations (15%, 30%, 50%, 70%, 95%, and 3× absolute ethanol). The dehydrated samples were embedded in Spurr's resin (Electron Microscopy Sciences). Ultrathin (90-nm) sections were cut with an ultramicrotome (EM [UC6]; Leica). The sections were observed using a JEOL JEM-1400 Plus transmission electron microscope.

Statistics. Statistical differences were determined by applying a two-sided Student *t* test using GraphPad Prism 6 at a *P* significance level of <0.05. Data are presented as means ± standard deviations.

SUPPLEMENTAL MATERIAL

Supplemental material for this article may be found at https://doi.org/10.1128/JVI.00749-17.

SUPPLEMENTAL FILE 1, PDF file, 0.1 MB.
SUPPLEMENTAL FILE 2, MP4 file, 0.4 MB.
SUPPLEMENTAL FILE 3, MP4 file, 0.8 MB.
SUPPLEMENTAL FILE 4, MP4 file, 0.2 MB.
SUPPLEMENTAL FILE 5, MP4 file, 0.7 MB.

ACKNOWLEDGMENTS

We thank Leigh Anne Olsen and Lynn Enquist (Princeton University, Princeton, NJ, USA) for their kind gift of anti-PRV US3 monoclonal antibodies, Bruno Verhasselt (Ghent University, Ghent, Belgium) for the pTrip plasmid, and the ID-DLO (The Netherlands) for the NIA3 PRV strains.

The research was supported by grants from the F.W.O.-Vlaanderen (Research Project G.0196.17N), the Hercules Foundation (Project AUGE/11/009), and Ghent University (Concerted Research Action BOF17-GOA-013).

REFERENCES

1. Rustom A, Saffrich R, Markovic I, Walther P, Gerdes H-H. 2004. Nanotubular highways for intercellular organelle transport. Science 303:1007–1010. https://doi.org/10.1126/science.1093133.
2. Onfelt B, Nedvetzki S, Yanagi K, Davis DM. 2004. Cutting edge: membrane nanotubes connect immune cells. J Immunol 173:1511–1513. https://doi.org/10.4049/jimmunol.173.3.1511.
3. Gerdes H-H, Rustom A, Wang X. 2013. Tunneling nanotubes, an emerging intercellular communication route in development. Mech Dev 130:381–387. https://doi.org/10.1016/j.mod.2012.11.006.
4. Abounit S, Zurzolo C. 2012. Wiring through tunneling nanotubes—from electrical signals to organelle transfer. J Cell Sci 125:1089–1098. https://doi.org/10.1242/jcs.083279.
5. Sisakhtnezhad S, Khosravi L. 2015. Emerging physiological and pathological implications of tunneling nanotubes formation between cells. Eur J Cell Biol 94:429–443. https://doi.org/10.1016/j.ejcb.2015.06.010.
6. Islam MN, Das SR, Emin MT, Wei M, Sun L, Westphalen K, Rowlands DJ, Quadri SK, Bhattacharya S, Bhattacharya J. 2012. Mitochondrial transfer from bone-marrow-derived stromal cells to pulmonary alveoli protects against acute lung injury. Nat Med 18:759–765. https://doi.org/10.1038/nm.2736.
7. Wang X, Veruki ML, Bukoreshtliev NV, Hartveit E, Gerdes H-H. 2010. Animal cells connected by nanotubes can be electrically coupled through interposed gap-junction channels. Proc Natl Acad Sci U S A 107:17194–17199. https://doi.org/10.1073/pnas.1006785107.
8. Domert J, Rao SB, Agholme L, Brorsson AC, Marcusson J, Hallbeck M, Nath S. 2014. Spreading of amyloid-beta peptides via neuritic cell-to-cell transfer is dependent on insufficient cellular clearance. Neurobiol Dis 65:82–92. https://doi.org/10.1016/j.nbd.2013.12.019.
9. Costanzo M, Abounit S, Marzo L, Danckaert A, Chamoun Z, Roux P, Zurzolo C. 2013. Transfer of polyglutamine aggregates in neuronal cells occurs in tunneling nanotubes. J Cell Sci 126:3678–3685. https://doi.org/10.1242/jcs.126086.
10. Gousset K, Zurzolo C. 2009. Tunnelling nanotubes: a highway for prion spreading? Prion 3:94–98. https://doi.org/10.4161/pri.3.2.8917.
11. Pasquier J, Galas L, Boulangé-Lecomte C, Rioult D, Bultelle F, Magal P, Webb G, Le Foll F. 2012. Different modalities of intercellular membrane exchanges mediate cell-to-cell P-glycoprotein transfers in MCF-7 breast cancer cells. J Biol Chem 287:7374–7387. https://doi.org/10.1074/jbc.M111.312157.
12. Sowinski S, Jolly C, Berninghausen O, Purbhoo MA, Chauveau A, Köhler K, Oddos S, Eissmann P, Brodsky FM, Hopkins C, Onfelt B, Sattentau Q, Davis DM. 2008. Membrane nanotubes physically connect T cells over long distances presenting a novel route for HIV-1 transmission. Nat Cell Biol 10:211–219. https://doi.org/10.1038/ncb1682.
13. Eugenin EA, Gaskill PJ, Berman JW. 2009. Tunneling nanotubes (TNT) are induced by HIV-infection of macrophages: a potential mechanism for intercellular HIV trafficking. Cell Immunol 254:142–148. https://doi.org/10.1016/j.cellimm.2008.08.005.
14. Roberts KL, Manicassamy B, Lamb RA. 2015. Influenza A virus uses intercellular connections to spread to neighboring cells. J Virol 89:1537–1549. https://doi.org/10.1128/JVI.03306-14.
15. Kumar A, Kim JH, Ranjan P, Metcalfe MG, Cao W, Mishina M, Gangappa S, Guo Z, Boyden ES, Zaki S, York I, García-Sastre A, Shaw M, Sambhara S. 2017. Influenza virus exploits tunneling nanotubes for cell-to-cell spread. Sci Rep 7:40360. https://doi.org/10.1038/srep40360.
16. Guo R, Katz BB, Tomich JM, Gallagher T, Fang Y. 2016. Porcine reproductive and respiratory syndrome virus utilizes nanotubes for intercellular spread. J Virol 90:5163–5175. https://doi.org/10.1128/JVI.00036-16.
17. Martinez MG, Kielian M. 2016. Intercellular extensions are induced by the alphavirus structural proteins and mediate virus transmission. PLoS Pathog 12:e1006061. https://doi.org/10.1371/journal.ppat.1006061.
18. Favoreel HW, Van Minnebruggen G, Adriaensen D, Nauwynck HJ. 2005. Cytoskeletal rearrangements and cell extensions induced by the US3 kinase of an alphaherpesvirus are associated with enhanced spread. Proc Natl Acad Sci U S A 102:8990–8995. https://doi.org/10.1073/pnas.0409099102.
19. Loesing JB, Di Fiore S, Ritter K, Fischer R, Kleines M. 2009. Epstein-Barr virus BDLF2-BMRF2 complex affects cellular morphology. J Gen Virol 90:1440–1449. https://doi.org/10.1099/vir.0.009571-0.
20. Gill MB, Edgar R, May JS, Stevenson PG. 2008. A gamma-herpesvirus glycoprotein complex manipulates actin to promote viral spread. PLoS One 3:e1808. https://doi.org/10.1371/journal.pone.0001808.
21. Ladelfa MF, Kotsias F, Del Médico Zajac MP, Van den Broeke C, Favoreel H, Romera SA, Calamante G. 2011. Effect of the US3 protein of bovine

herpesvirus 5 on the actin cytoskeleton and apoptosis. Vet Microbiol 153:361–366. https://doi.org/10.1016/j.vetmic.2011.05.037.
22. Finnen RL, Roy BB, Zhang H, Banfield BW. 2010. Analysis of filamentous process induction and nuclear localization properties of the HSV-2 serine/threonine kinase Us3. Virology 397:23–33. https://doi.org/10.1016/j.virol.2009.11.012.
23. Van den Broeke C, Radu M, Deruelle M, Nauwynck H, Hofmann C, Jaffer ZM, Chernoff J, Favoreel HW. 2009. Alphaherpesvirus US3-mediated reorganization of the actin cytoskeleton is mediated by group A p21-activated kinases. Proc Natl Acad Sci U S A 106:8707–8712. https://doi.org/10.1073/pnas.0900436106.
24. Jacob T, Van den Broeke C, Van Waesberghe C, Van Troys L, Favoreel HW. 2015. Pseudorabies virus US3 triggers RhoA phosphorylation to reorganize the actin cytoskeleton. J Gen Virol 96:2328–2335. https://doi.org/10.1099/vir.0.000152.
25. Austefjord MW, Gerdes HH, Wang X. 2014. Tunneling nanotubes: diversity in morphology and structure. Commun Integr Biol 7:e27934. https://doi.org/10.4161/cib.27934.
26. McCoy-Simandle K, Hanna SJ, Cox D. 2016. Exosomes and nanotubes: control of immune cell communication. Int J Biochem Cell Biol 71:44–54. https://doi.org/10.1016/j.biocel.2015.12.006.
27. Janke C, Chloë Bulinski J. 2011. Post-translational regulation of the microtubule cytoskeleton: mechanisms and functions. Nat Rev Mol Cell Biol 12:773–786. https://doi.org/10.1038/nrm3227.
28. Paturle-Lafanechère L, Manier M, Trigault N, Pirollet F, Mazarguil H, Job D. 1994. Accumulation of delta 2-tubulin, a major tubulin variant that cannot be tyrosinated, in neuronal tissues and in stable microtubule assemblies. J Cell Sci 107:1529–1543.
29. Takeichi M. 2014. Dynamic contacts: rearranging adherens junctions to drive epithelial remodelling. Nat Rev Mol Cell Biol 15:397–410. https://doi.org/10.1038/nrm3802.
30. Rauh I, Mettenleiter TC. 1991. Pseudorabies virus glycoproteins gII and gp50 are essential for virus penetration. J Virol 65:5348–5356.
31. Ahmad T, Mukherjee S, Pattnaik B, Kumar M, Singh S, Rehman R, Tiwari BK, Jha KA, Barhanpurkar AP, Wani MR, Roy SS, Mabalirajan U, Ghosh B, Agrawal A. 2014. Miro1 regulates intercellular mitochondrial transport & enhances mesenchymal stem cell rescue efficacy. EMBO J 33:994–1010.
32. Wang X, Gerdes H-H. 2015. Transfer of mitochondria via tunneling nanotubes rescues apoptotic PC12 cells. Cell Death Differ 22:1181–1191. https://doi.org/10.1038/cdd.2014.211.
33. Marzo L, Gousset K, Zurzolo C. 2012. Multifaceted roles of tunneling nanotubes in intercellular communication. Front Physiol 3:72. https://doi.org/10.3389/fphys.2012.00072.
34. Hammond JW, Cai D, Verhey KJ. 2008. Tubulin modifications and their cellular functions. Curr Opin Cell Biol 20:71–76. https://doi.org/10.1016/j.ceb.2007.11.010.
35. Song Y, Brady ST. 2015. Post-translational modifications of tubulin: pathways to functional diversity of microtubules. Trends Cell Biol 25:125–136. https://doi.org/10.1016/j.tcb.2014.10.004.
36. Naghavi MH, Gundersen GG, Walsh D. 2013. Plus-end tracking proteins, CLASPs, and a viral Akt mimic regulate herpesvirus-induced stable microtubule formation and virus spread. Proc Natl Acad Sci U S A 110:18268–18273. https://doi.org/10.1073/pnas.1310760110.
37. Lokar M, Iglic A, Veranic P. 2010. Protruding membrane nanotubes: Attachment of tubular protrusions to adjacent cells by several anchoring junctions. Protoplasma 246:81–87. https://doi.org/10.1007/s00709-010-0143-7.
38. Astanina K, Koch M, Jüngst C, Zumbusch A, Kiemer AK. 2015. Lipid droplets as a novel cargo of tunnelling nanotubes in endothelial cells. Sci Rep 5:11453. https://doi.org/10.1038/srep11453.
39. Gerdes HH, Carvalho RN. 2008. Intercellular transfer mediated by tunneling nanotubes. Curr Opin Cell Biol 20:470–475. https://doi.org/10.1016/j.ceb.2008.03.005.
40. Kramer T, Enquist LW. 2012. Alphaherpesvirus infection disrupts mitochondrial transport in neurons. Cell Host Microbe 11:504–514. https://doi.org/10.1016/j.chom.2012.03.005.
41. Peeters B, de Wind N, Hooisma M, Wagenaar F, Gielkens A, Moormann R. 1992. Pseudorabies virus envelope glycoproteins gp50 and gII are essential for virus penetration, but only gII is involved in membrane fusion. J Virol 66:894–905.
42. de Wind N, Zijderveld A, Glazenburg K, Gielkens A, Berns A. 1990. Linker insertion mutagenesis of herpesviruses: inactivation of single genes within the Us region of pseudorabies virus. J Virol 64:4691–4696.
43. Kimman TG, De Wind N, Oei-Lie N, Pol JMA, Berns AJM, Gielkens ALJ. 1992. Contribution of single genes within the unique short region of Aujeszky's disease virus (suid herpesvirus type 1) to virulence, pathogenesis and immunogenicity. J Gen Virol 73:243–251. https://doi.org/10.1099/0022-1317-73-2-243.
44. Jacob T, Van den Broeke C, van Troys M, Waterschoot D, Ampe C, Favoreel HW. 2013. Alphaherpesviral US3 kinase induces cofilin dephosphorylation to reorganize the actin cytoskeleton. J Virol 87:4121–4126. https://doi.org/10.1128/JVI.03107-12.
45. Geenen K, Favoreel HW, Olsen L, Enquist LW, Nauwynck HJ. 2005. The pseudorabies virus US3 protein kinase possesses anti-apoptotic activity that protects cells from apoptosis during infection and after treatment with sorbitol or staurosporine. Virology 331:144–150. https://doi.org/10.1016/j.virol.2004.10.027.
46. Deruelle M, Geenen K, Nauwynck HJ, Favoreel HW. 2007. A point mutation in the putative ATP binding site of the pseudorabies virus US3 protein kinase prevents Bad phosphorylation and cell survival following apoptosis induction. Virus Res 128:65–70. https://doi.org/10.1016/j.virusres.2007.04.006.
47. Olsen LM, Ch'ng TH, Card JP, Enquist LW. 2006. Role of pseudorabies virus Us3 protein kinase during neuronal infection. J Virol 80:6387–6398. https://doi.org/10.1128/JVI.00352-06.
48. Nauwynck HJ, Pensaert MB. 1995. Effect of specific antibodies on the cell-associated spread of pseudorabies virus in monolayers of different cell types. Arch Virol 140:1137–1146. https://doi.org/10.1007/BF01315422.